

Electronic Supplementary Information

Cyclododecene isomeric separation by (supported) rhodium(I)- catalysed selective dehydrogenative borylation reaction

Amravati S. Singh and Antonio Leyva-Pérez.*

Instituto de Tecnología Química (UPV-CSIC), Universidad Politècnica de València–
Consejo Superior de Investigaciones Científicas, Avda. de los Naranjos s/n, 46022
Valencia, Spain.

Corresponding author e-mail: anleyva@itq.upv.es. Phone: +34963877812; Fax:
+34963877809.

Index.

Experimental Section.....	ESI2
General.	ESI2
Physical techniques.	ESI2
Additional reaction procedures.	ESI3
Figures S1–S28.....	ESI5

Experimental Section.

– General.

Glassware was dried in an oven at 175 °C before use. Reagents and solvents were obtained from commercial sources and were used without further purification otherwise indicated. Catalysts, products and intermediates were characterized by gas chromatography– mass spectrometry and ^1H , ^{13}C , ^{31}P , ^{11}B and DEPT liquid nuclear magnetic resonance, and the resulting spectra compared with the given literature.

– Physical techniques.

Inductively coupled plasma-atomic emission spectroscopy (ICP-AES). The metal content of the zeolites was determined after disaggregating the solids in aqueous HF and dilution before analysis.

Gas chromatography-mass spectrometry (GC-MS). Gas chromatographic analyses were performed in an instrument equipped with a 25 cm capillary column of 5% phenylmethylsilicone. *N*-dodecane was used as an external standard. Gas chromatography–mass spectrometry analyses were performed on a spectrometer equipped with the same column as the GC and operated under the same conditions.

Nuclear magnetic resonance (NMR). ^1H , ^{13}C , ^{31}P , ^{11}B and distortionless enhancement by polarization transfer (DEPT) liquid nuclear magnetic resonance (NMR) measurements, and also bidimensional ^1H - ^1H NMR, were recorded on a 400 MHz Bruker Avance instrument at room temperature, using deuterated chloroform or toluene- d^8 as a solvent, which contains or not TMS as an internal standard.

X-ray diffraction (XRD). Spectra were recorded in a CubiX PRO (PAN Analytical) spectrometer, with a Cu K(α) radiation source, 1.5406 Å wavelength.

Fourier transformed infrared spectroscopy (FT-IR). Spectra were recorded on attenuated total reflection infrared spectroscopy, from 400 to 4000 cm^{-1} , by dropping a small sample of the solid on the ATR crystal, or dissolving the Rh complex, dropping the solution and leaving to evaporate the organic solvent for a few minutes.

Diffuse reflectance ultraviolet visible spectrophotometry (DR-UVvis). Absorption spectra of the solids were recorded on a spectrophotometer under diffuse reflectance mode.

X-ray photoelectron spectroscopy (XPS). Measurements were performed on a SPECS spectrometer equipped with a Phoibos 150 MCD-9 analyser using a non-monochromatic Mg KR (1,253.6 eV) X-ray source working at 50 W. The C1s peak has been set at 284.5 eV as the internal reference for the peak positions in the XPS spectra.

Field emission scanning electron microscopy (FESEM). The sample was supported on a grid and measured with a ZEISS Ultra-55 instrument, from Oxford Instruments.

Electron microscopy characterization. Images of the zeolite catalyst samples were obtained on a JEM-F2100 operated at 200 kV in dark field scanning transmission electron microscopy (DF-STEM mode), with EDS instrumentation.

Solid state magic angle spinning nuclear magnetic resonance (SS-MAS NMR). The ^{27}Al spectra were recorded at room temperature in a Bruker AVIII HD 400 WB spectrometer, with $\pi/12$ pulse length of 1 μs , and a recycle delay of 3 s, pinning the samples at 20 kHz. The ^{29}Si spectra were recorded at room temperature in a Bruker BL7 7 mm probe spectrometer, with $\pi/12$ pulse length of $<500 \mu\text{s}$, and a recycle delay of 60 s, pinning the samples at 5 kHz.

Ultra-performance liquid chromatography-high-resolution mass spectrum (UPLC-HRMS). The NMR sample (aprox. 20 μL) was diluted in 1 mL of UPLC-grade acetonitrile containing 0.1% (v:v) of acetic acid, filtered and analyzed by direct infusion in positive mode.

Additional reaction procedures.

Hot filtration test. Reagent **1** (*cis/trans* 73:27 cyclododecene mixture, 0.3 mmol), (BPin)₂ (2 equiv.) in toluene (0.5M) and the solid catalyst (90 mg, unless otherwise indicated) were introduced in a sealed vial with a magnetic stirrer. The mixture was allowed to react for 1 h at 100 °C. GC samples were prepared taking out 50 μL of the supernatant, and introducing them in a vial with 0.5 mL of toluene and *N*-dodecane (11 μL , 0.05 mmol) as an external standard. After this time, the solid catalyst was removed by filtration, and the filtrates were placed in another vial at the reaction temperature under similar stirring, to also follow the reaction without solid catalyst. The kinetic results between the reaction with solid catalyst or not were compared (see Figure S20 ahead).

Reuse of the solid catalyst. The first use was carried out following the above described procedure. Then, after completion of the reaction, the solid catalyst was centrifuged and

washed at least three times with dichloromethane. The solid was dried under vacuum and used for the next reaction, adding the corresponding amounts of reagents.

Figures.

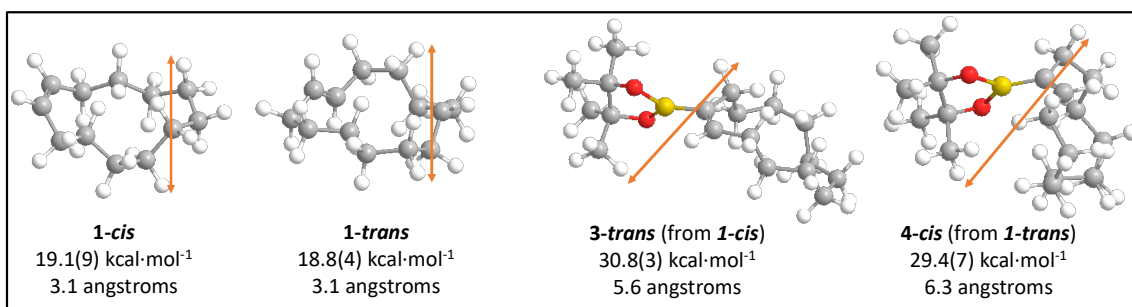


Figure S1. Molecular mechanics calculations (MM2) in the vacuum for the *cis* and *trans* isomers of cyclododecene (**1-cis** and **1-trans**, respectively) and the corresponding dehydrogenative monoborylated products (**3-trans** and **3-cis**, respectively; the latter is barely produced during the reaction here), showing the free energy and the kinetic radius for all of them. The orange arrows indicate the minimum distance between two atoms in any spatial direction (kinetic radius). Colour code: C atoms (grey), H atoms (white), O atoms (red) and B atoms (yellow).

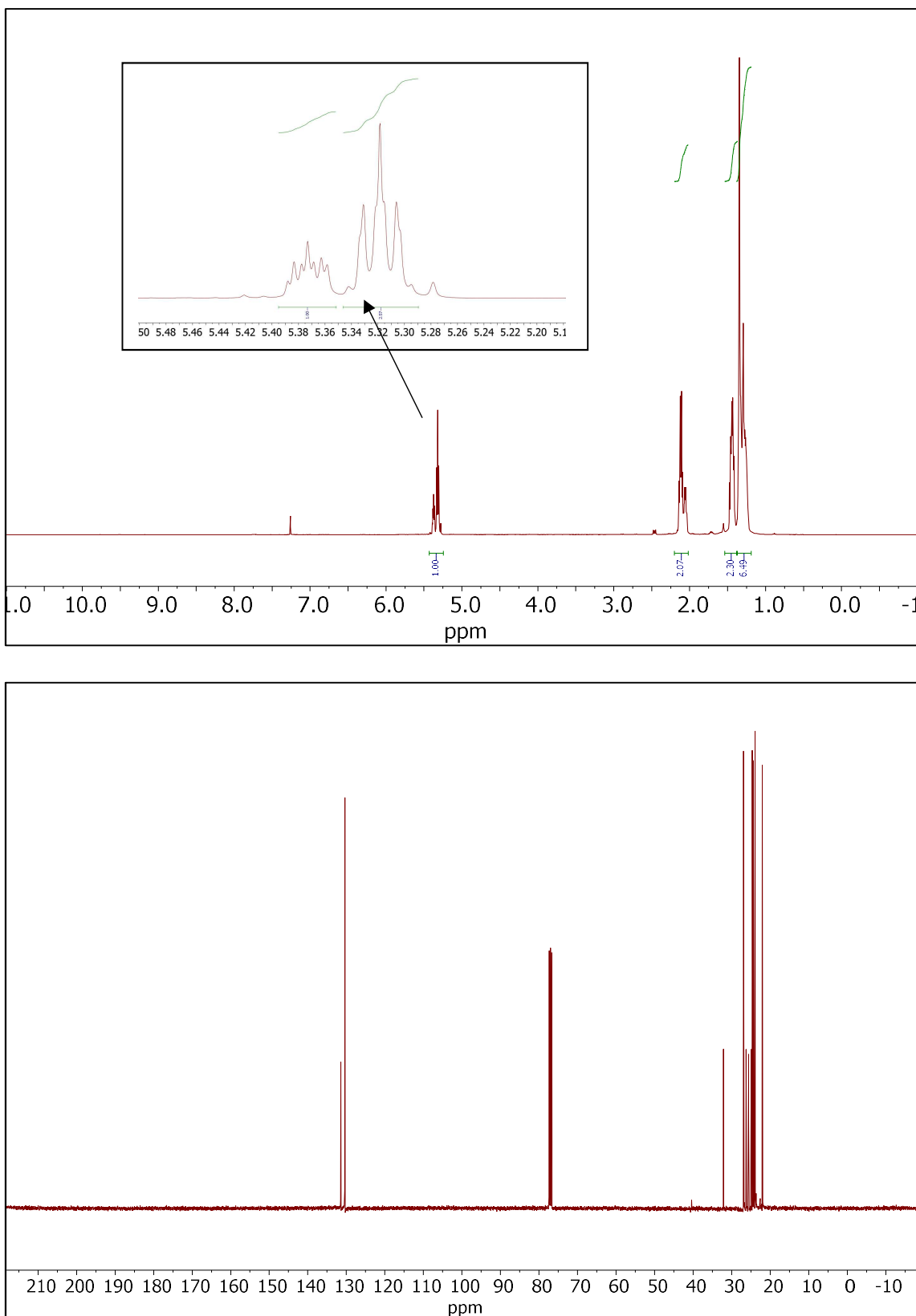
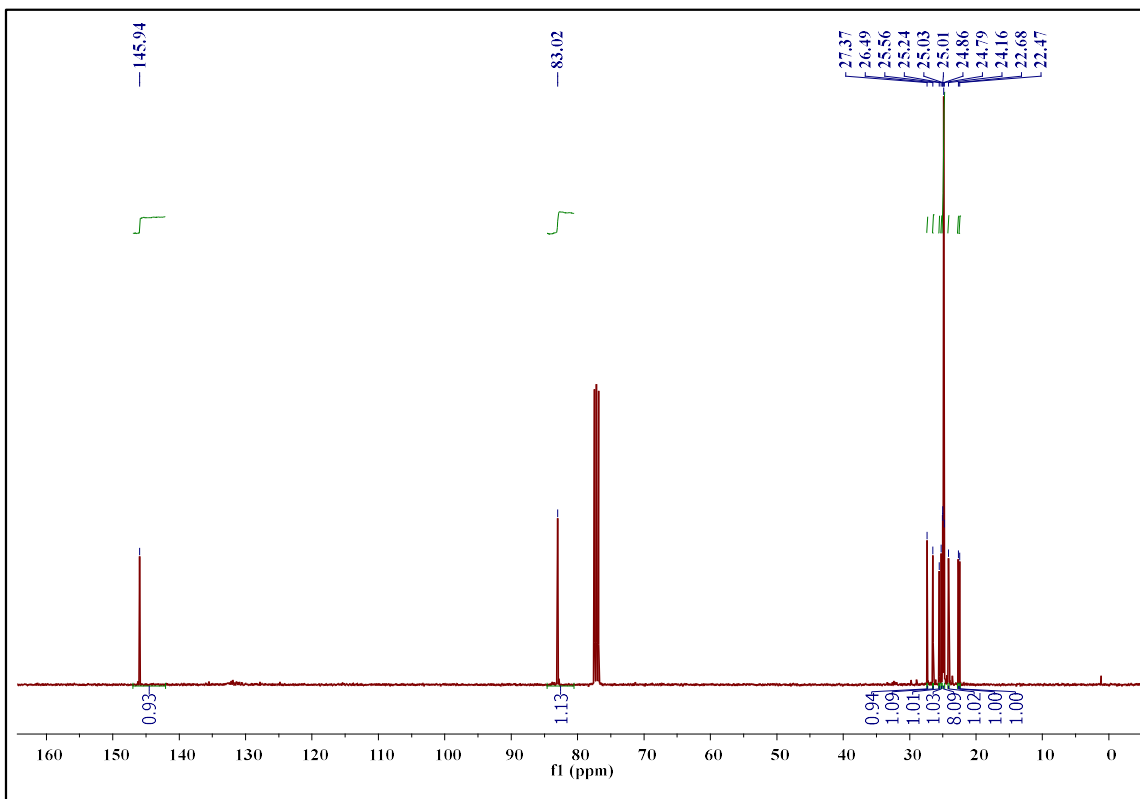
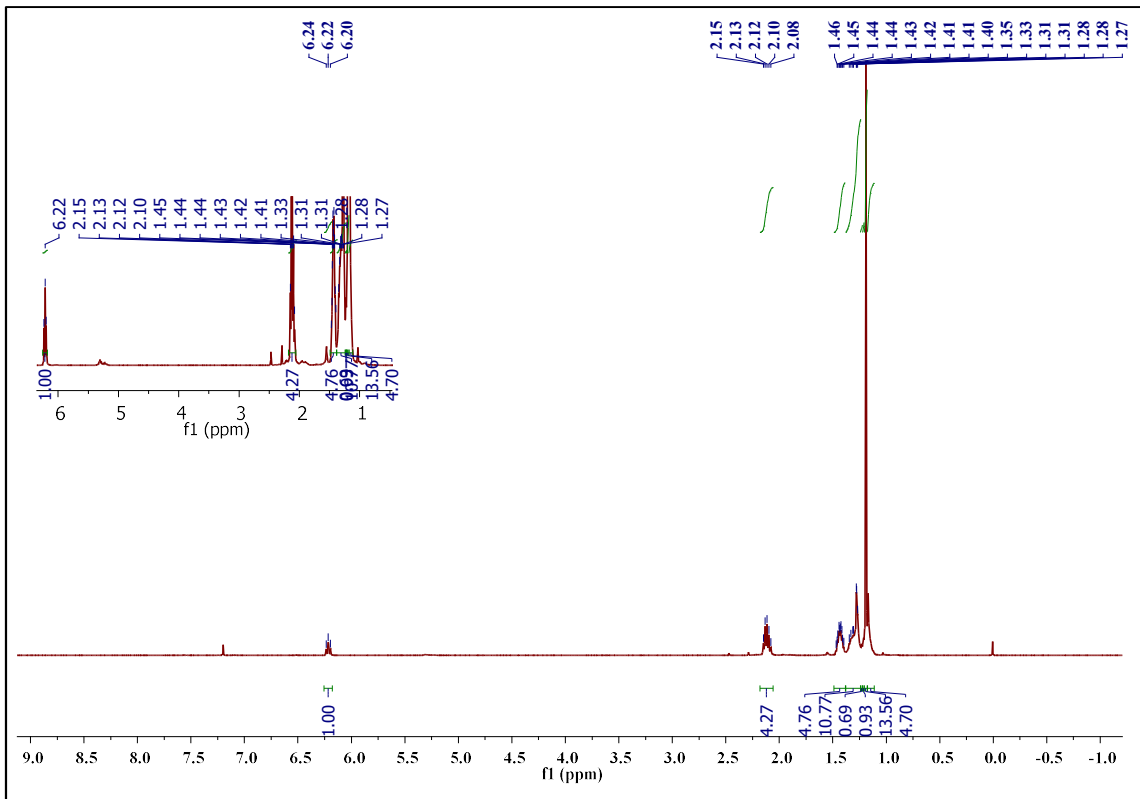


Figure S2. Top: ¹H NMR spectrum of the commercially available cyclododecene **1** *cis/trans* mixture (73:27), the inset shows the diagnostic alkene signals. Bottom: the corresponding ¹³C NMR spectrum.



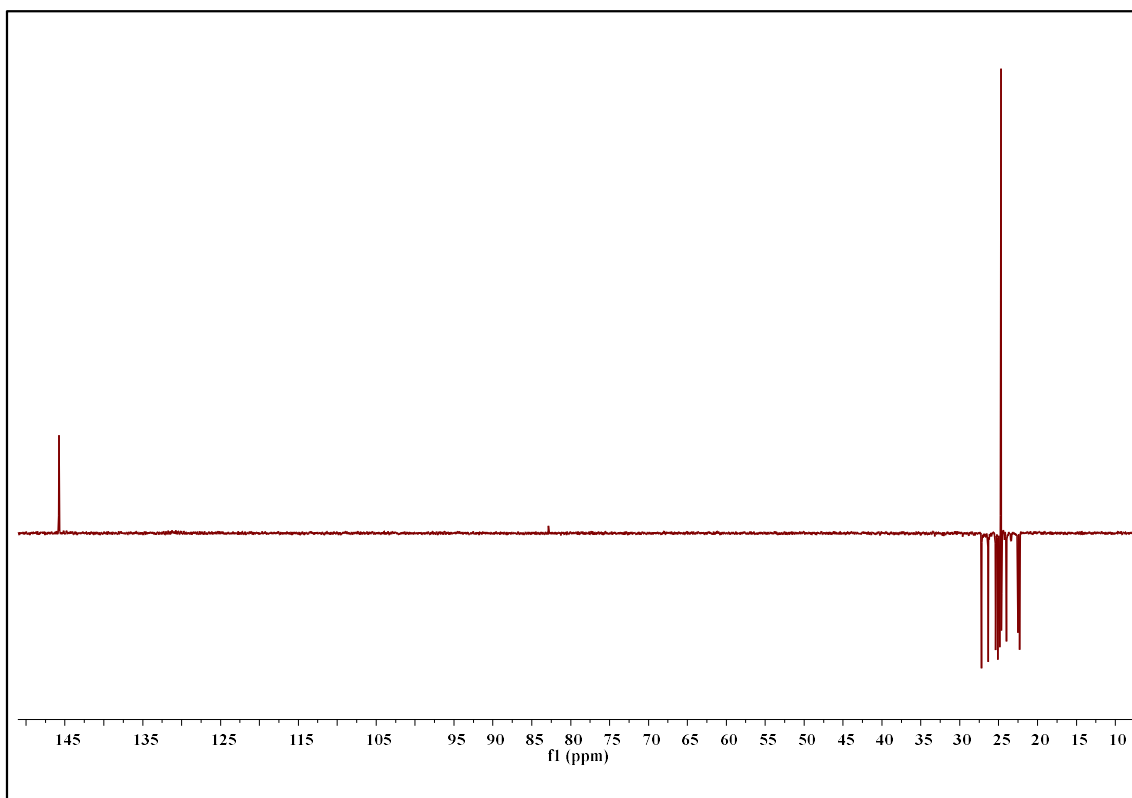
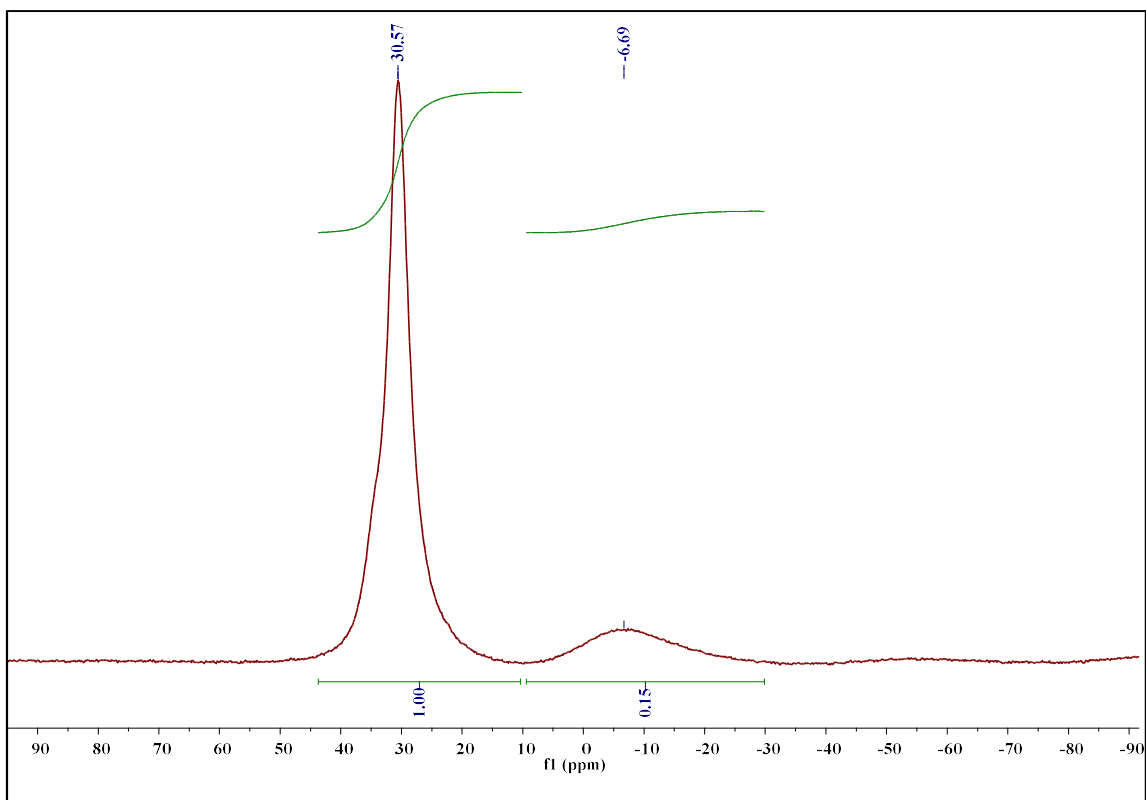
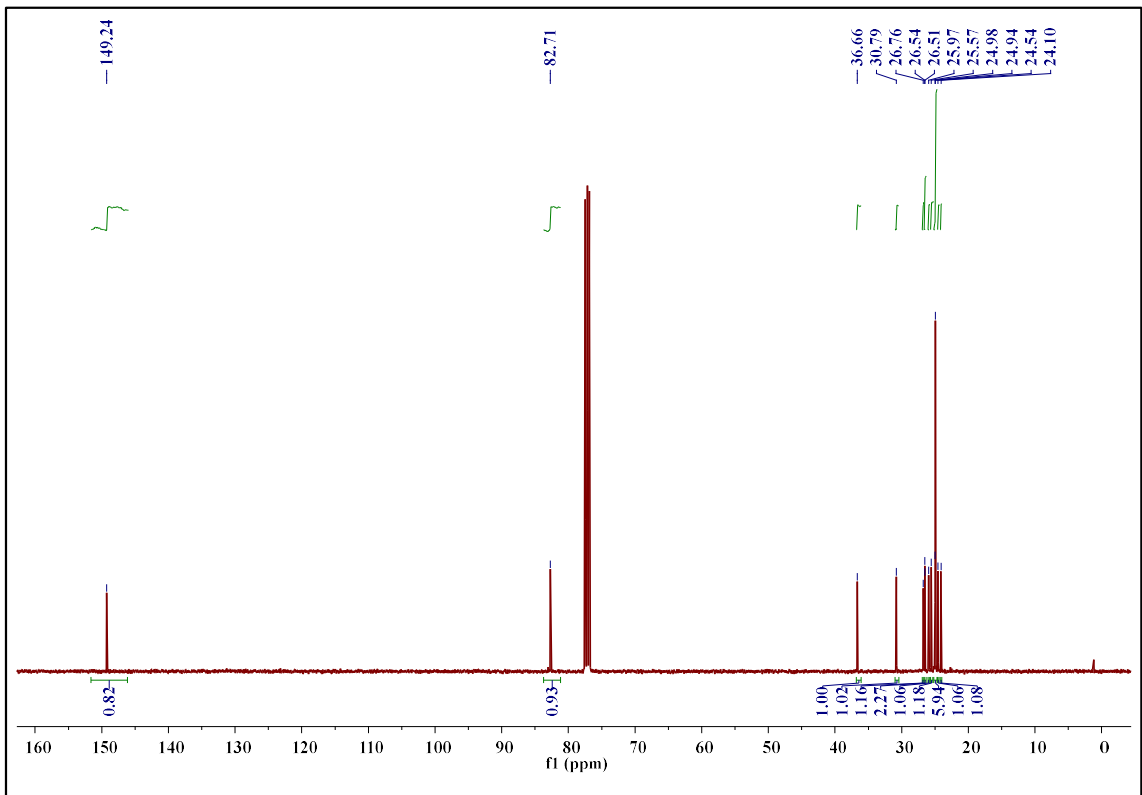
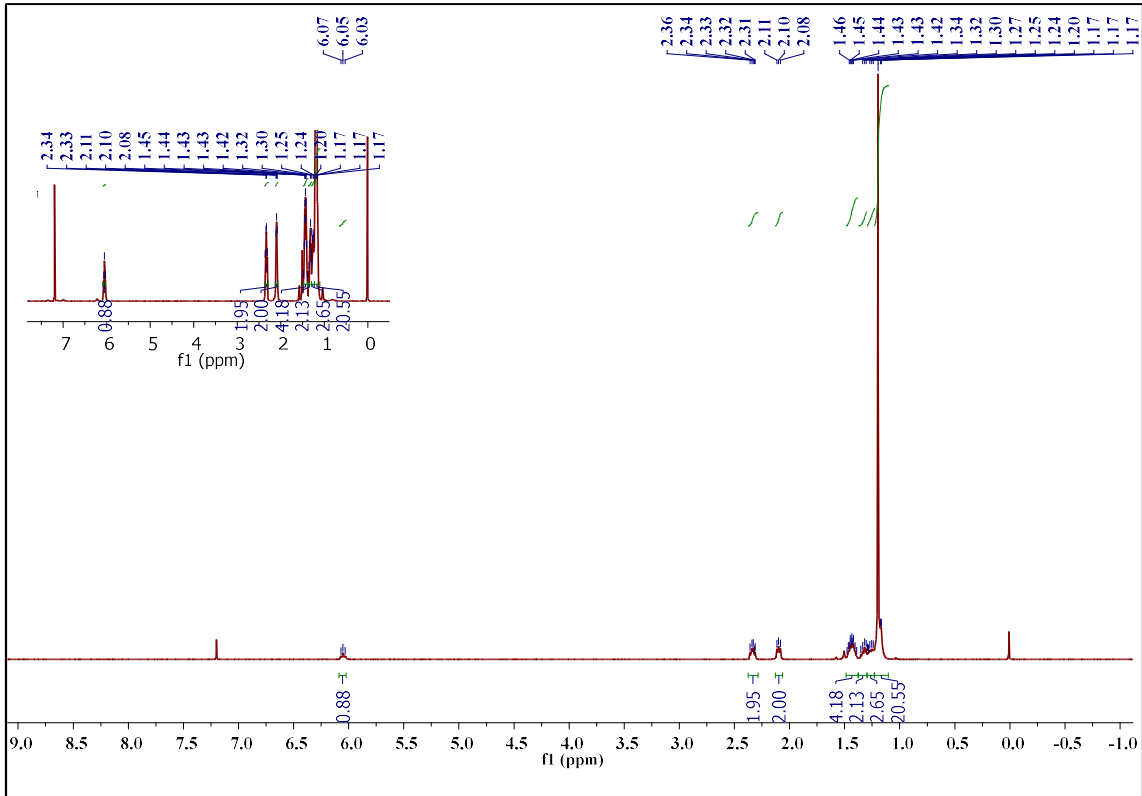


Figure S3. From top to bottom: ^1H , ^{13}C and ^{11}B nuclear magnetic resonance (NMR) and DEPT spectra of pure **3**. GC-MS (m/z , M^+ :292), major peaks found: 292(100%), 277, 235, 207, 164, 153,121, 101, 83, 55, 29. ^1H NMR (401 MHz, CDCl_3) δ 6.22 (t, $J = 7.8$

Hz, 1H), 2.18 – 2.05 (m, 4H), 1.43 (dtd, $J = 13.6, 6.9, 4.3$ Hz, 5H), 1.38 – 1.24 (m, 11H), 1.24 – 1.18 (m, 15H), 1.17 (t, $J = 3.3$ Hz, 5H). ^{13}C NMR (101 MHz, CDCl_3) δ 146.28 (s), 83.36 (s), 27.71 (s), 26.83 (s), 25.90 (s), 25.58 (s), 25.26 (dd, $J = 19.1, 4.7$ Hz), 24.50 (s), 23.02 (s), 22.81 (s). ^{11}B NMR (96 MHz, CDCl_3) δ 30.57 (s), -6.69 (s).



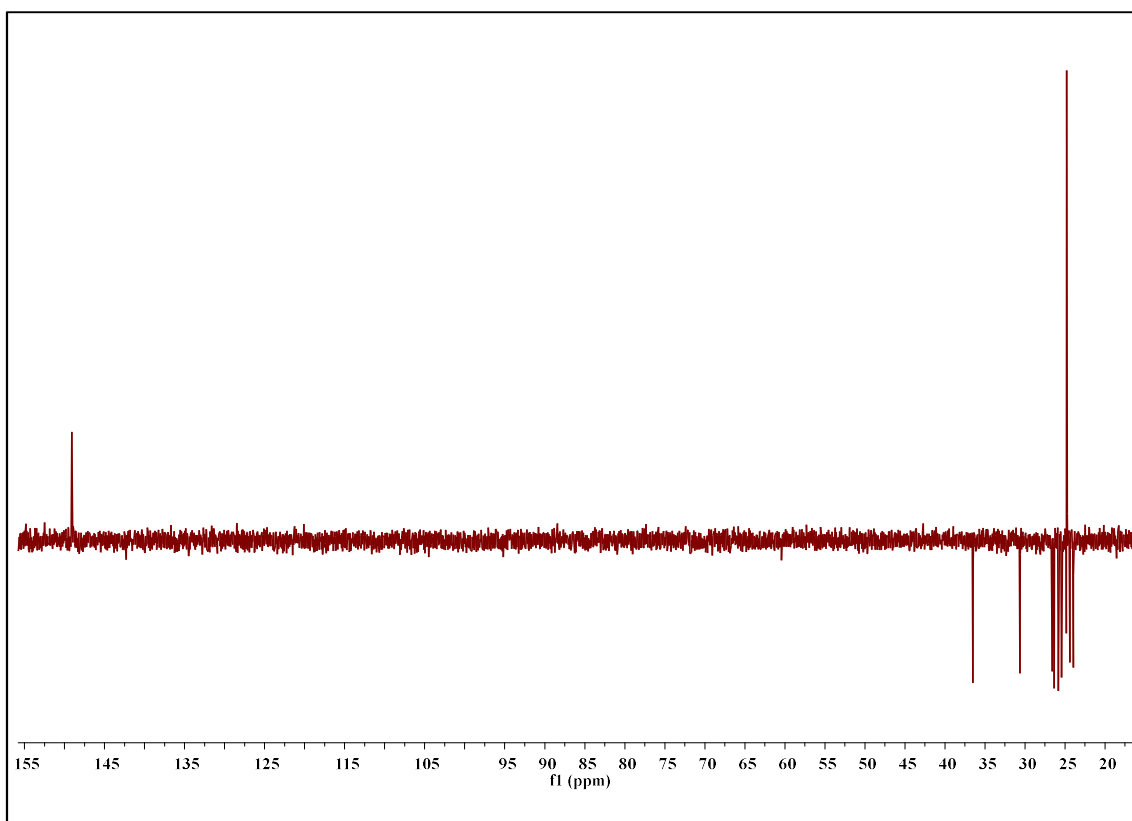
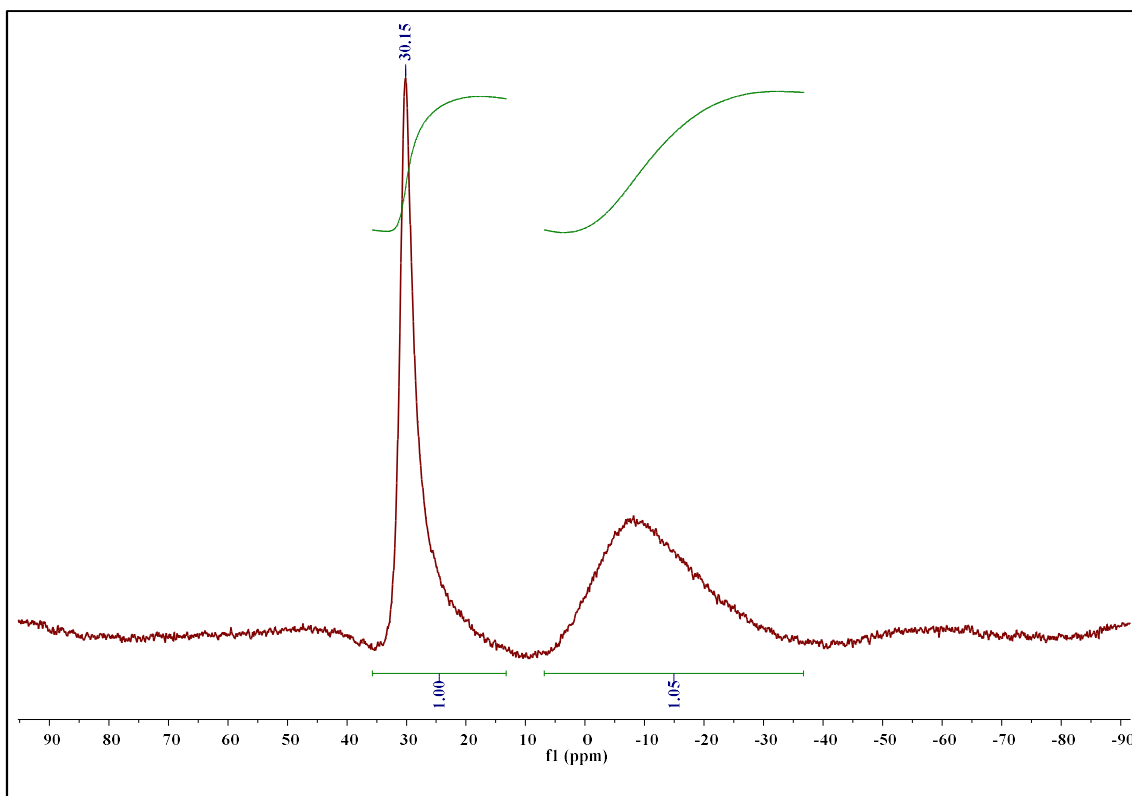


Figure S4. From top to bottom: ^1H , ^{13}C and ^{11}B nuclear magnetic resonance (NMR) and DEPT spectra of pure **4**. GC-MS (m/z , M^+ : 292), major peaks found: 292(100%), 277, 235, 207, 164, 149, 121, 101, 85, 55, 29. ^1H NMR (401 MHz, CDCl_3) δ 6.05 (t, $J = 7.8$

Hz, 1H), 2.38 – 2.29 (m, 2H), 2.15 – 2.06 (m, 2H), 1.49 – 1.38 (m, 5H), 1.33 (dd, $J = 12.8, 6.2$ Hz, 2H), 1.30 – 1.24 (m, 2H), 1.23 – 1.11 (m, 22H). ^{13}C NMR (101 MHz, CDCl_3) δ 149.58 (s), 83.05 (s), 37.00 (s), 31.13 (s), 27.10 (s), 26.87 (d, $J = 3.1$ Hz), 26.31 (s), 25.91 (s), 25.30 (d, $J = 4.1$ Hz), 24.88 (s), 24.44 (s). ^{11}B NMR (96 MHz, CDCl_3) δ 30.15 (s), 8.51 – -35.35 (m).

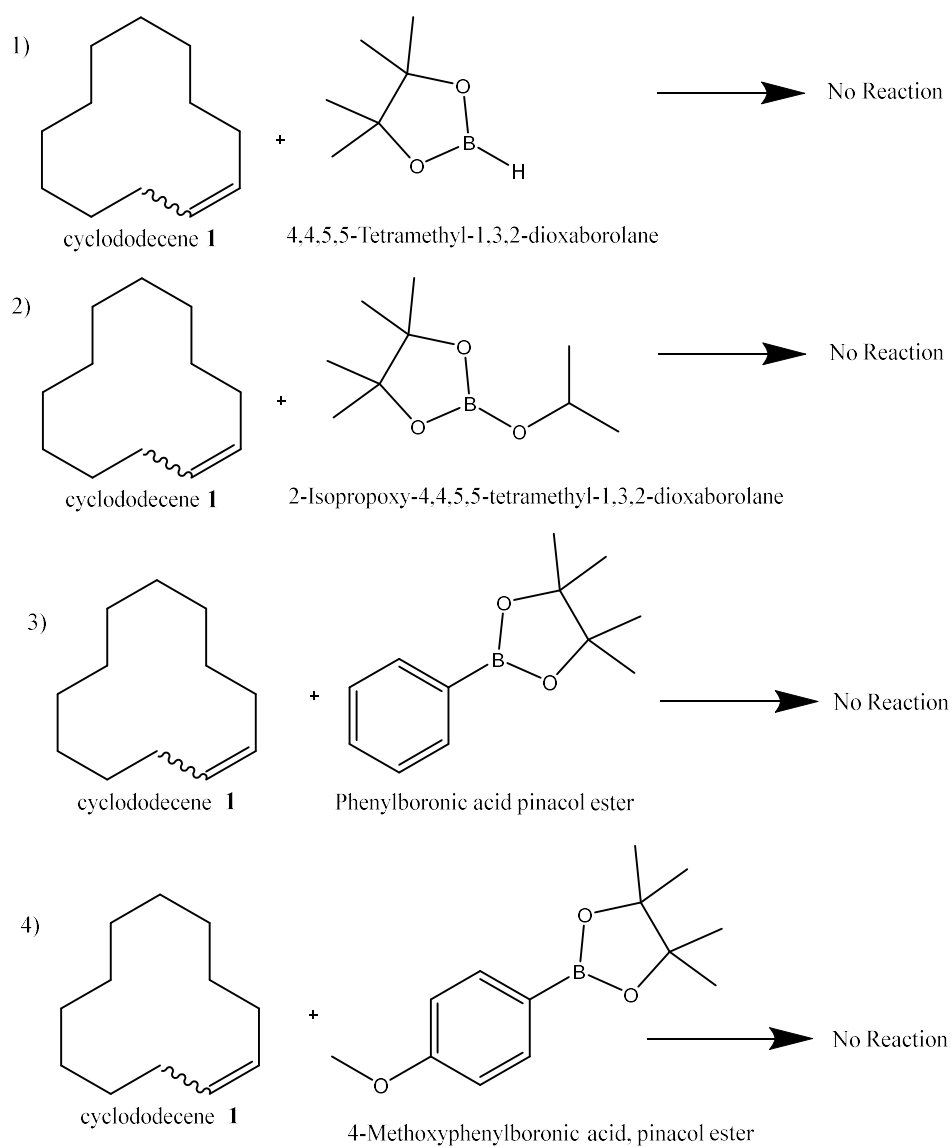


Figure S5. Unsuccessful reaction attempts with monoborylated reagents, under the optimized Rh-catalyzed reaction conditions in Table 1.

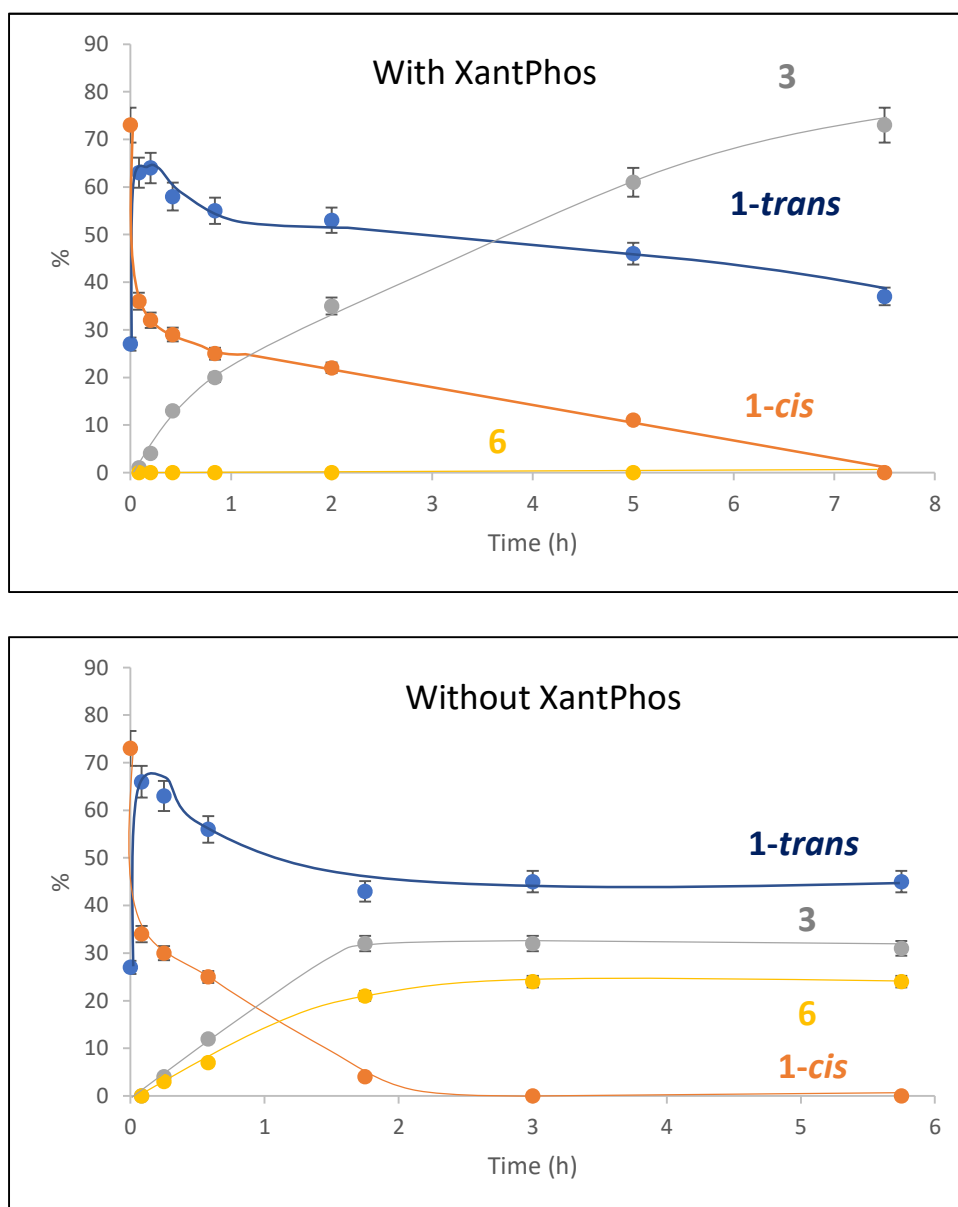


Figure S6. Kinetic plots for the dehydrogenative borylation reaction of the *cis/trans* (73:27) cyclododecene mixture **1** with (BPin)₂ **2** in toluene (0.5M) at 100 °C. Top: [Rh(COD)Cl]₂ (3 mol% of Rh) and XantPhos (6 mol%) as catalysts. Bottom: without XantPhos. Reactants and products are identified in different colors, as indicated, and the kinetic points for product **4** are not shown since values are <5%. Error bars account for a 5% uncertainty. Lines are a guide to the eye.

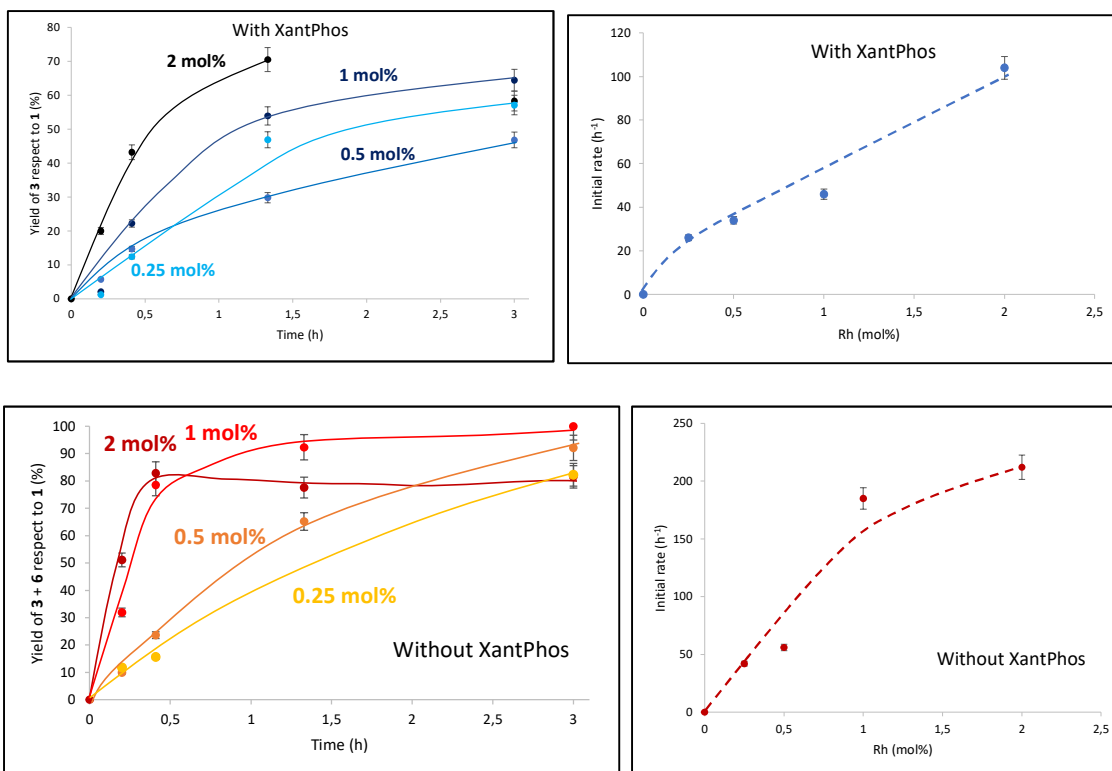


Figure S7. Kinetic plots (left) and reaction order (right) for Rh during the dehydrogenative borylation reaction of the *cis/trans* (73:27) cyclododecene mixture **1** with (BPin)₂ **2** in toluene (0.5M) at 100 °C. Top: [Rh(COD)Cl]₂ (3 mol% of Rh) and XantPhos (6 mol%) as catalysts. A linear correlation between initial rate and Rh mol% indicates first order in Rh. Bottom: without XantPhos. Error bars account for a 5% uncertainty. Lines are a guide to the eye.

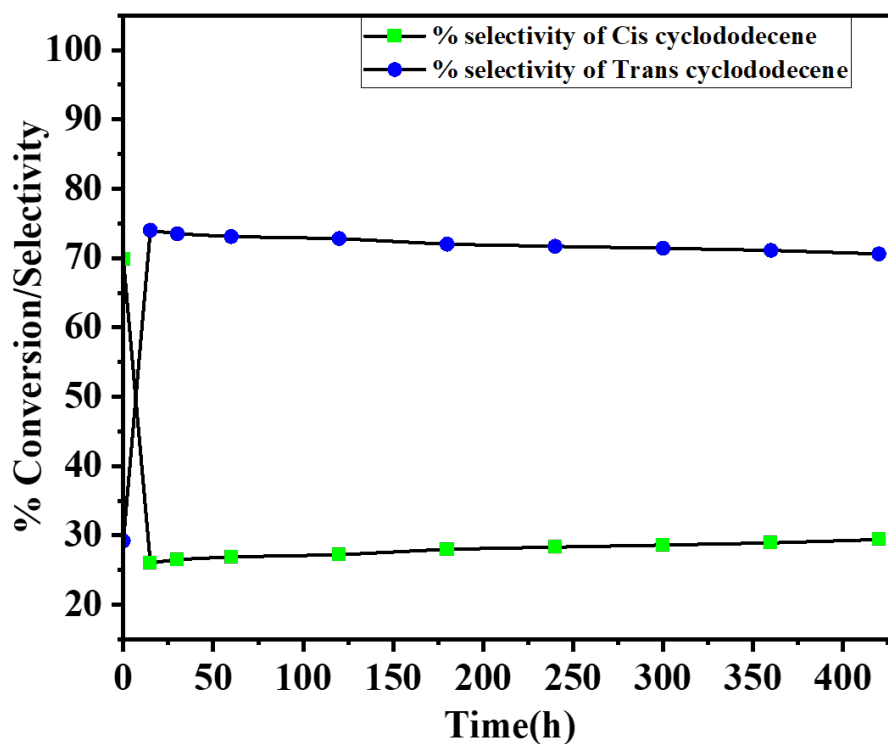
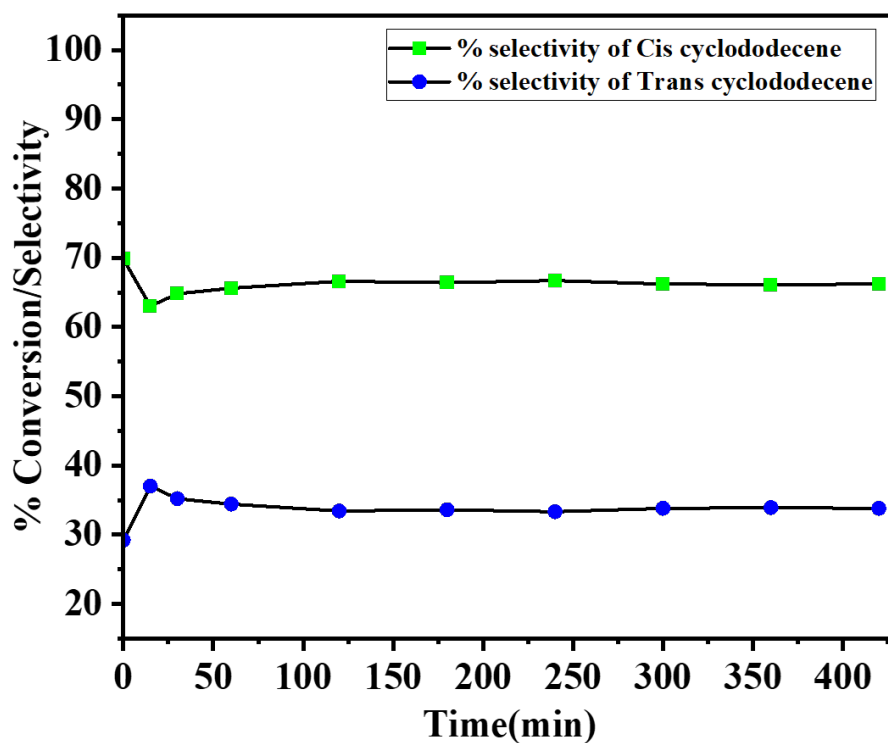


Figure S8. Kinetic study on the isomerization of the starting cyclododecene **1** mixture (73% cis, 27% trans), without reagent **2** in the medium, and with complex $[\text{Rh}(\text{COD})\text{Cl}]_2$ catalyst in the presence (top) or not (bottom) of the XantPhos ligand, under the optimized Rh-catalyzed reaction conditions in Table 1.

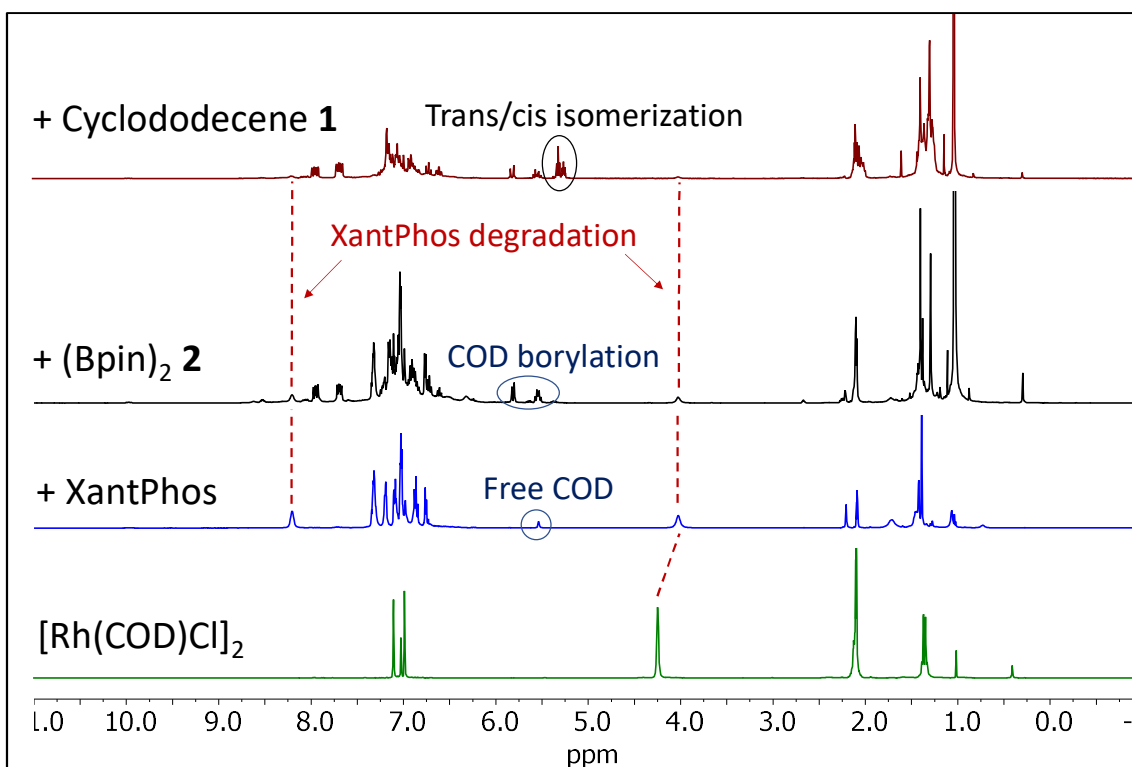


Figure S9. In-situ ^1H NMR measurements of the dehydrogenative borylation reaction of the *cis/trans* (73:27) cyclododecene mixture **1** with 2 equivalents of $(\text{BPin})_2$ **2** in toluene- d^8 (0.5M) at room temperature. Reactants were sequentially added from bottom to top.

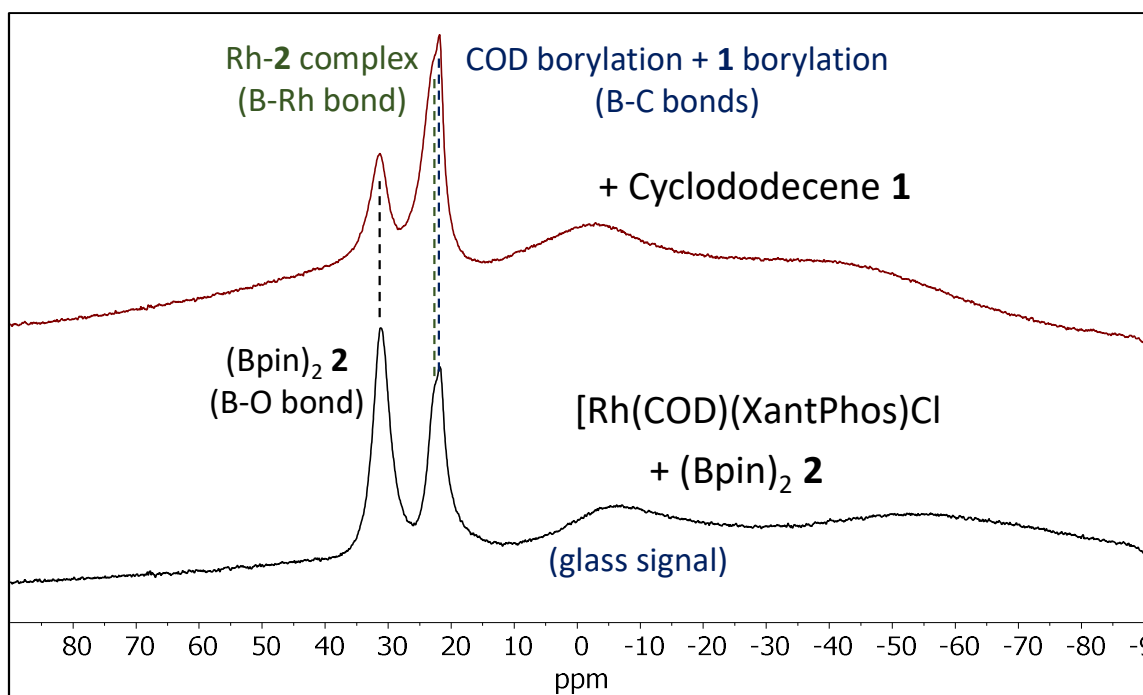


Figure S10. In-situ ^{11}B NMR measurements of the dehydrogenative borylation reaction of the *cis/trans* (73:27) cyclododecene mixture **1** with 2 equivalents of $(\text{BPin})_2$ **2** in toluene- d^8 (0.5M) at room temperature. Cyclododecene **1** is added to the mixture of catalyst and $(\text{BPin})_2$ **2**.

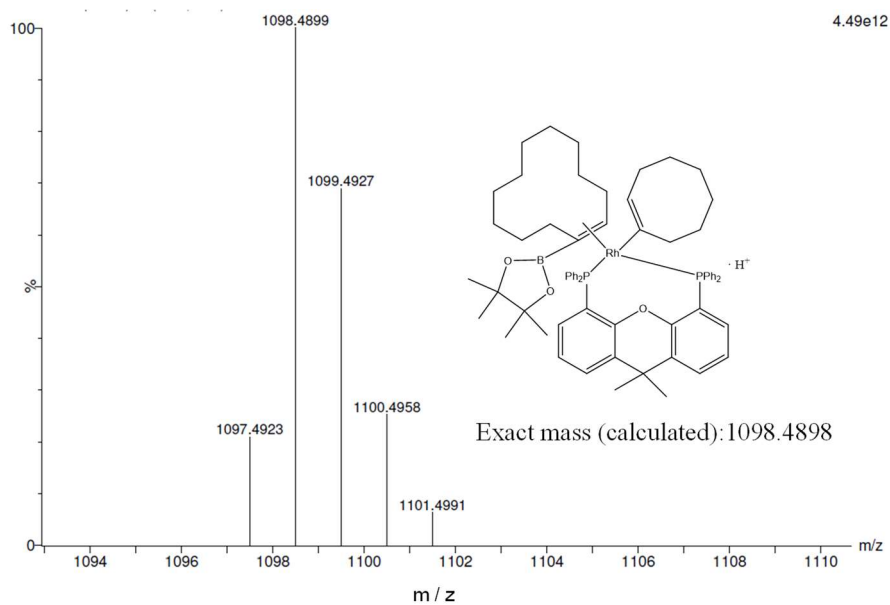


Figure S11. Diagnostic part of the ultra-performance liquid chromatography-high-resolution mass spectrum (UPLC-HRMS) after direct infusion of the NMR mixture studied in Figure 2. The species show different H atom ruptures.

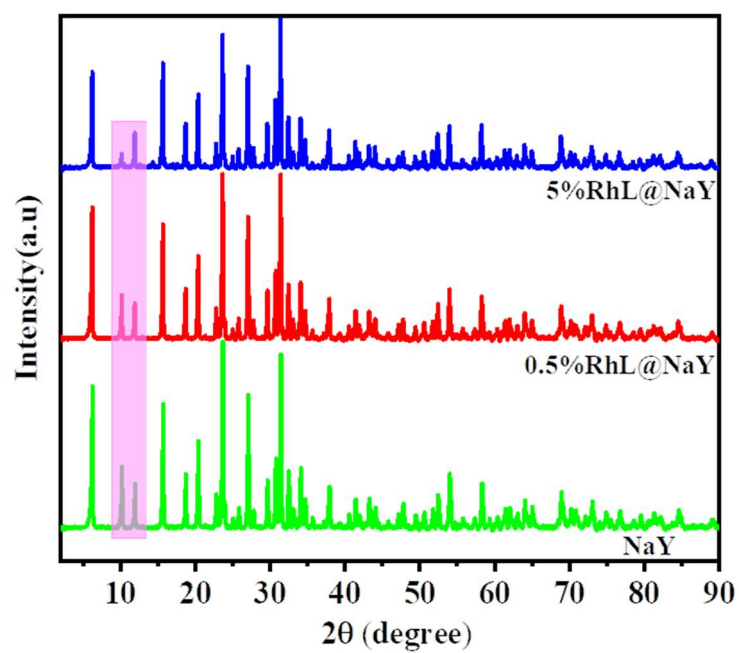


Figure S12. Powder X-ray diffraction (PXRD) of 0.5%RhL@NaY and 5%RhL@NaY compared to the pristine NaY zeolite.

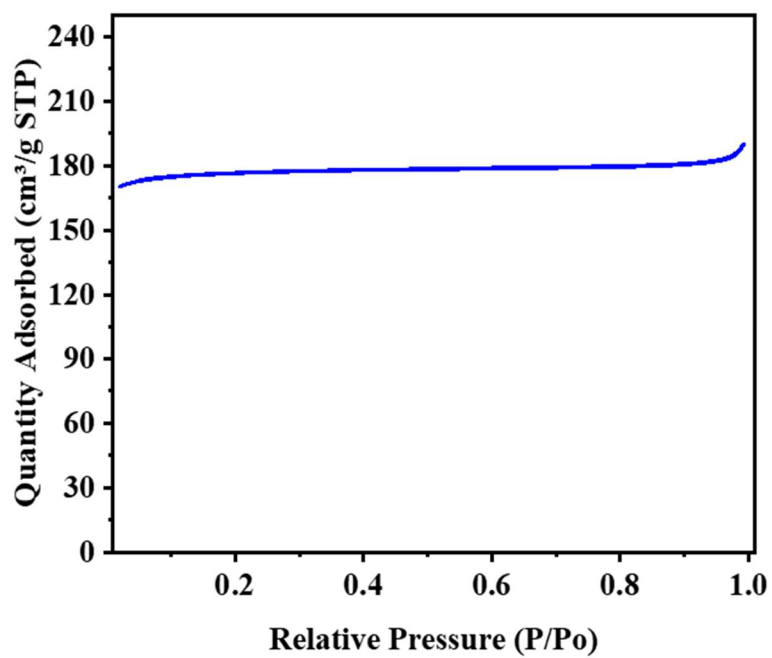


Figure S13. Brunauer-Emmett-Teller surface area (BET) measurement for 5%RhL@NaY.

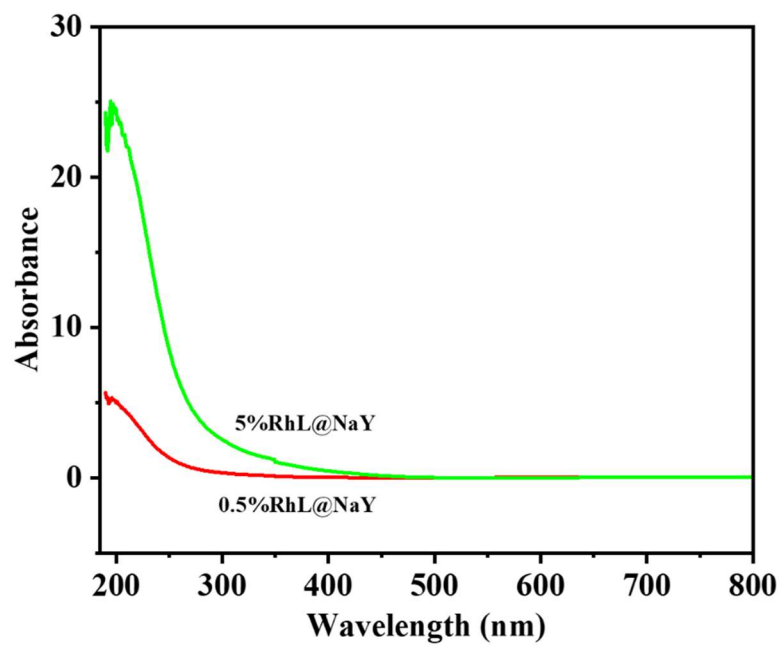


Figure S14. Diffuse-reflectance ultraviolet visible spectrophotometry (DR-UVvis) measurements for 0.5%RhL@NaY and 5%RhL@NaY.

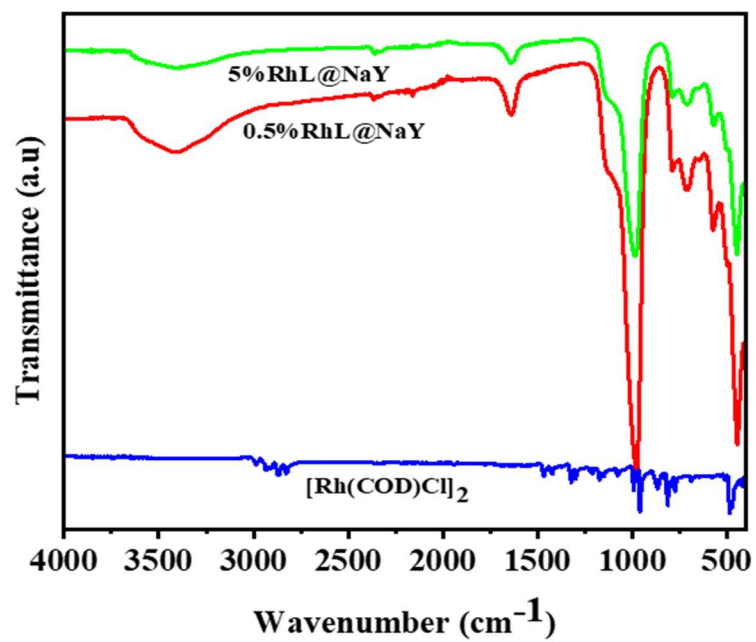


Figure S15. Fourier transformed infrared (FT-IR) spectra for 0.5%RhL@NaY and 5%RhL@NaY compared to the starting Rh complex.

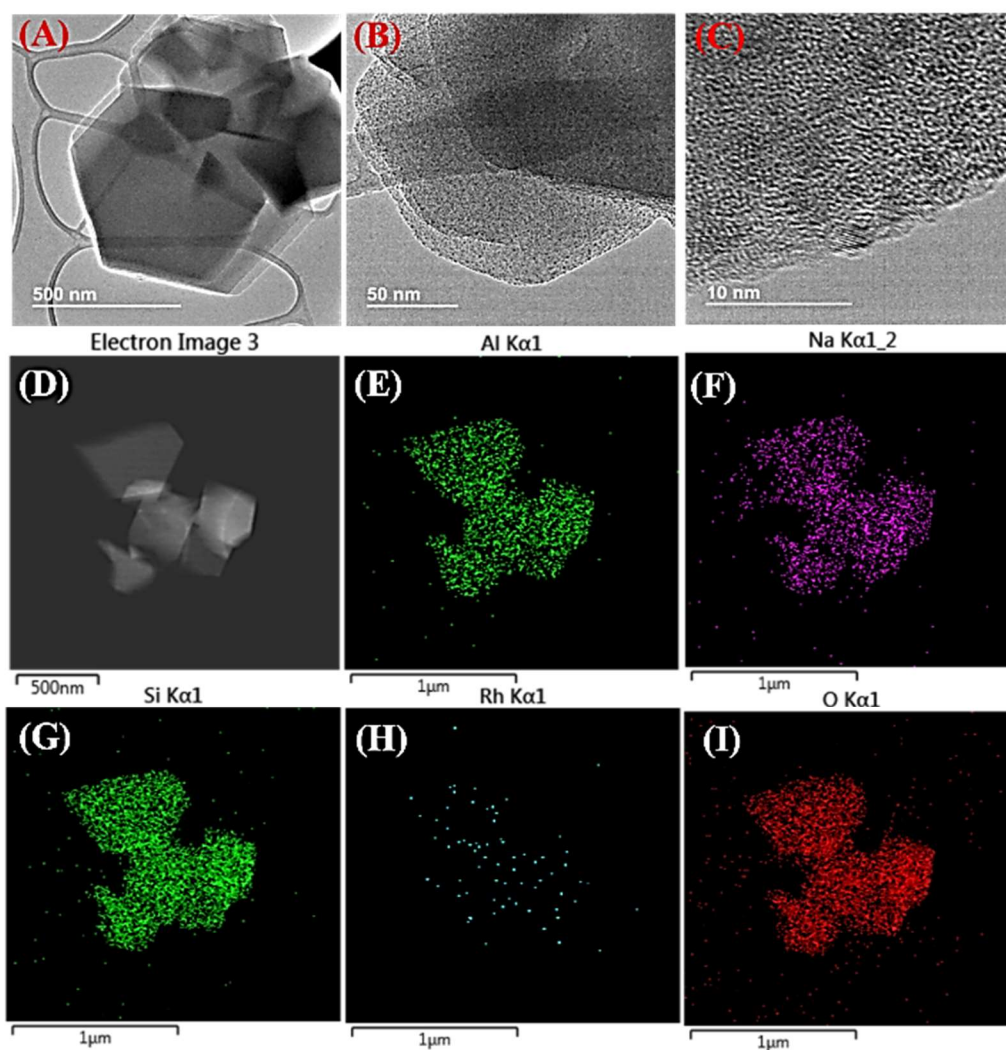
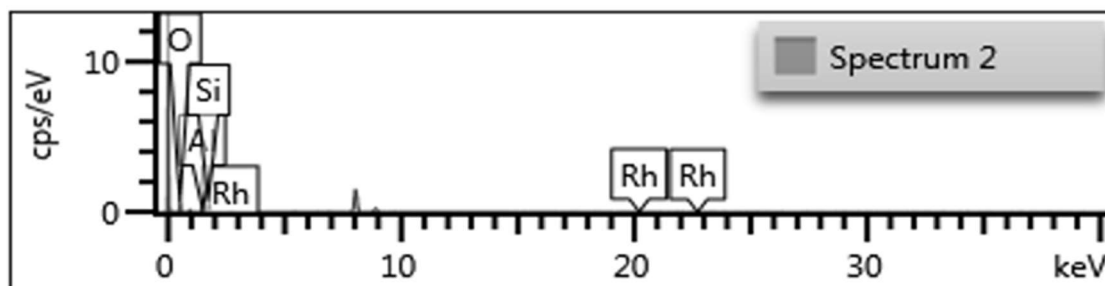


Figure S16. Representative images of 5%RhL@NaY by X-ray energy dispersive spectroscopy (EDS) coupled to high-angle-annular-dark field scanning transmission electron microscopy (HAADF-STEM). (A-C) TEM images, (D) electron images, (E-I) mapping images: (D) Aluminium, (F) Sodium, (G) Silicon, (H) Rhodium and (I) Oxygen.



Element	Line Type	k Factor	k Factor type	Absorption Correction	Wt%	Wt% Sigma	
O	K series	2.02	Theoretical		1	39.3	2.4
Al	K series	1.049	Theoretical		1	10.06	0.94
Si	K series	1	Theoretical		1	31.41	1.94
Rh	K series	7.601	Theoretical		1	19.23	3.98
Total:						100	

Figure S17. Elemental analysis of the surface of the 5%RhL@NaY solid according to HR-TEM EDX spectra.

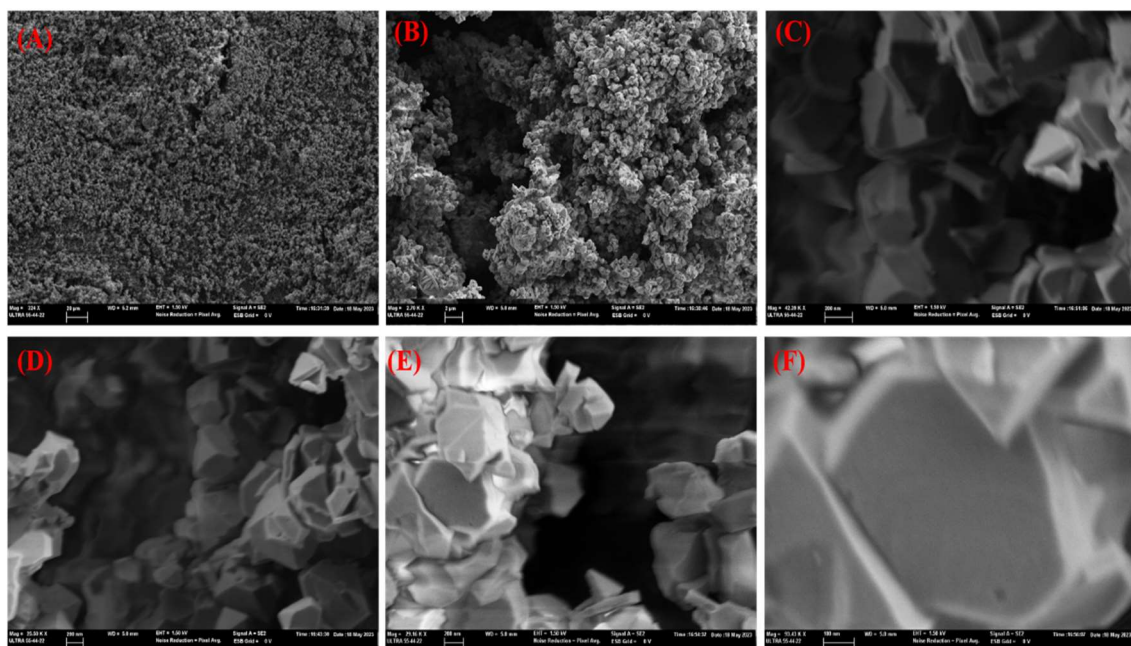


Figure S18. Field emission scanning electron microscope (FE-SEM) images of the 5%RhL@NaY solid.

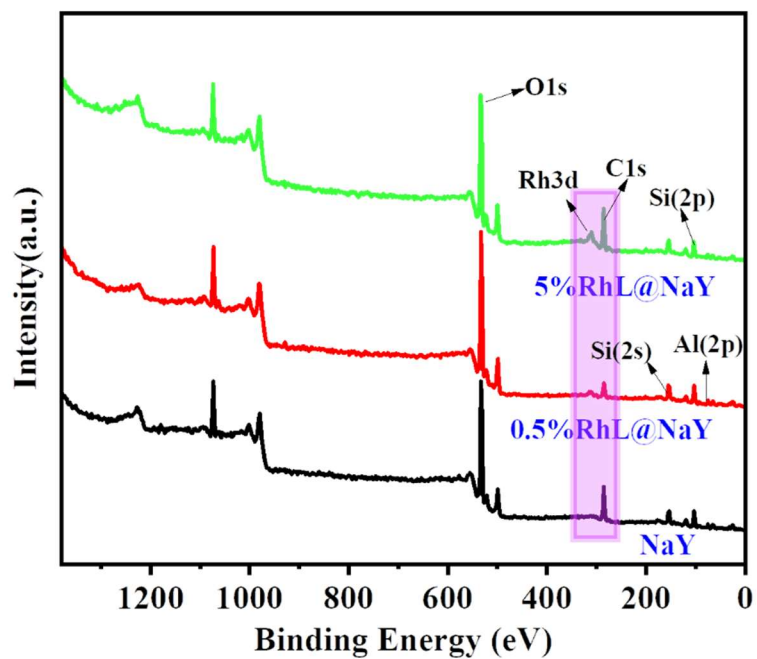


Figure S19. Comparison of the X-ray photoelectron spectrometry (XPS) survey spectra of 0.5%RhL@NaY, 5%RhL@NaY and zeolite NaY.

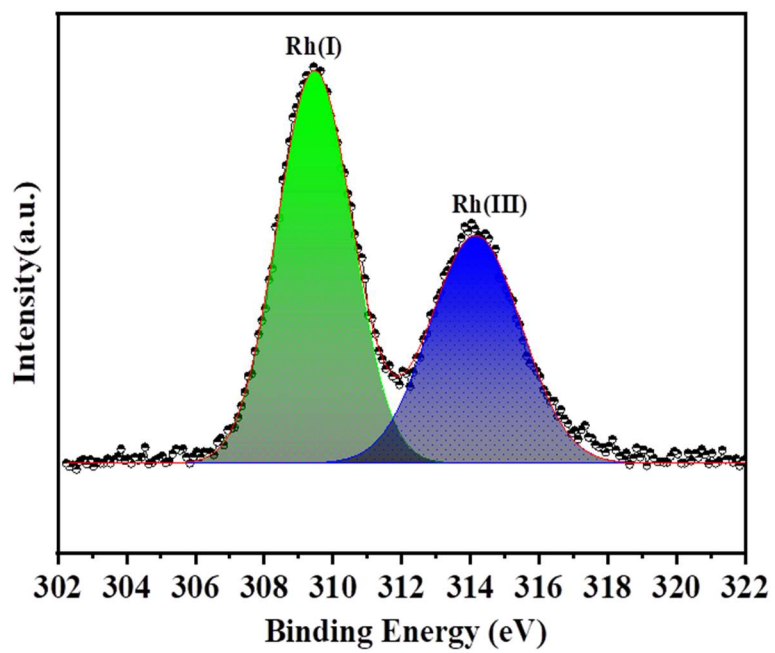


Figure S20. Rh 3d X-ray photoelectron spectroscopy (XPS) peaks of 0.5%Rh@NaY.

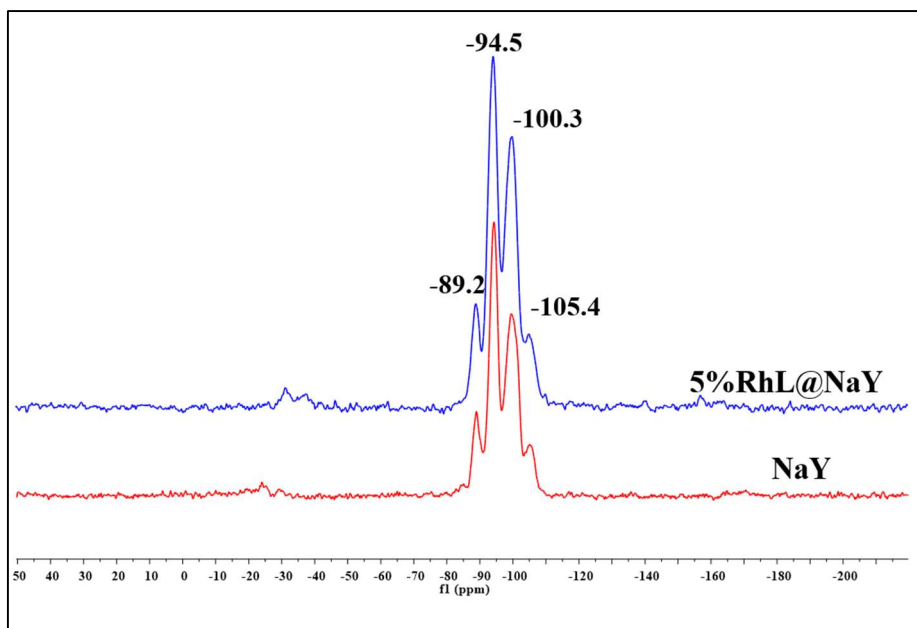


Figure S21. ^{29}Si solid-state magic angle spinning nuclear magnetic resonance (^{29}Si SS-MAS NMR) of 5%RhL@NaY and zeolite NaY.

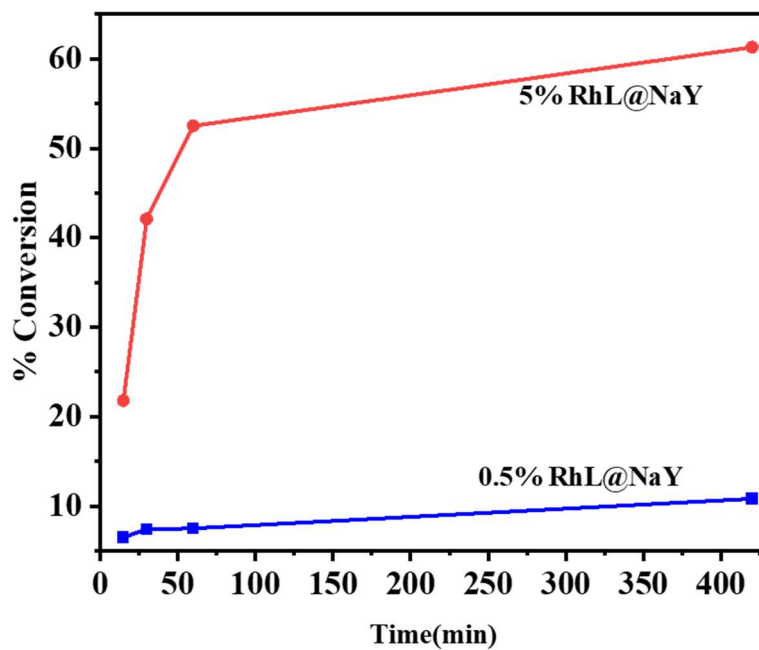


Figure S22. Catalytic comparison data for 0.5% and 5% RhL@NaY to evaluate that Rh(I) is the active species in the catalyst.

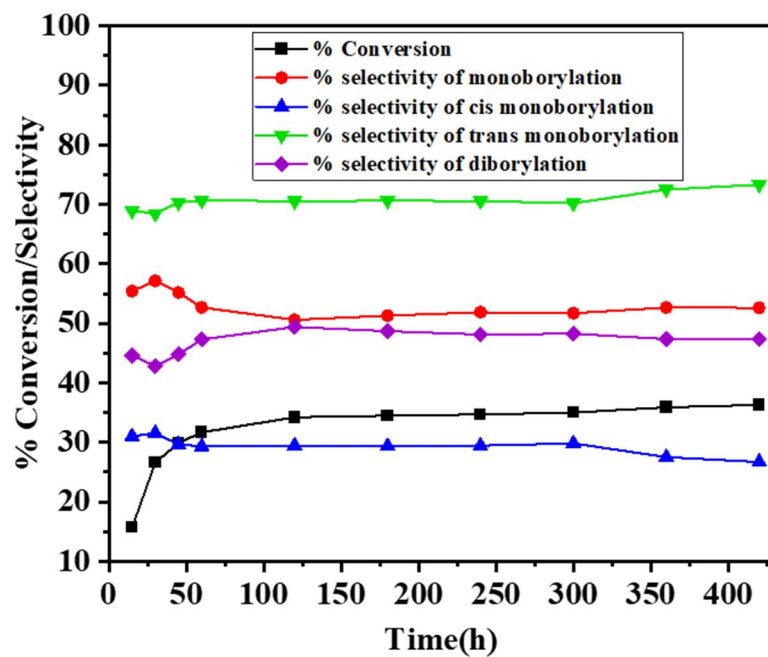


Figure S23. Hot filtration test. After 1 h reaction time, the 5%RhL@NaY catalyst was separated from the reaction mixture, and the reaction with the filtrates was also followed.

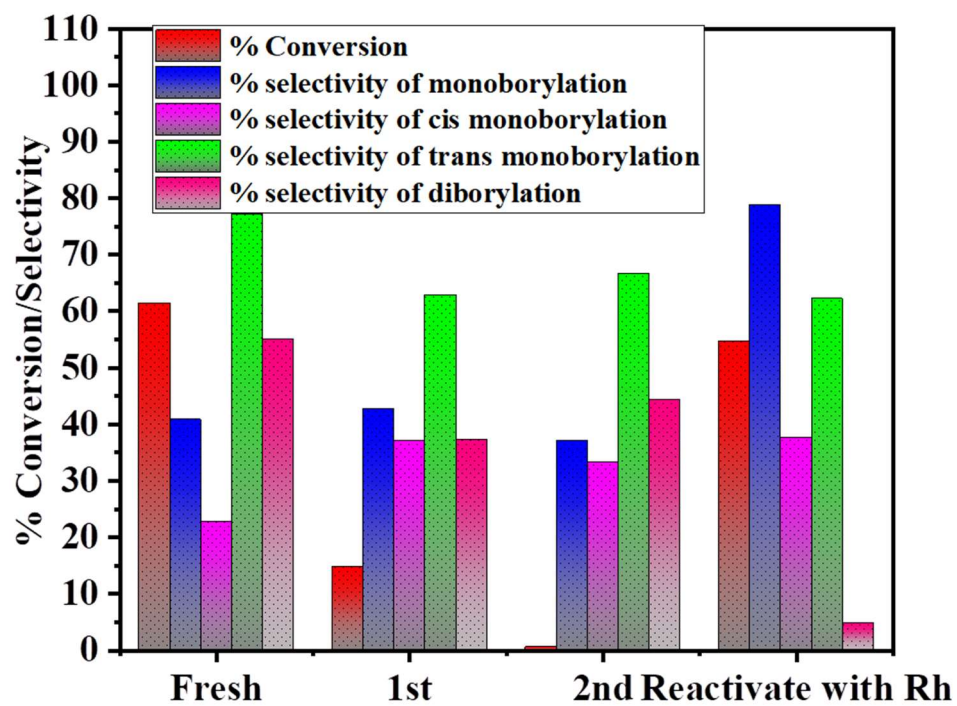


Figure S24. Recyclability test for 5%RhL@NaY.

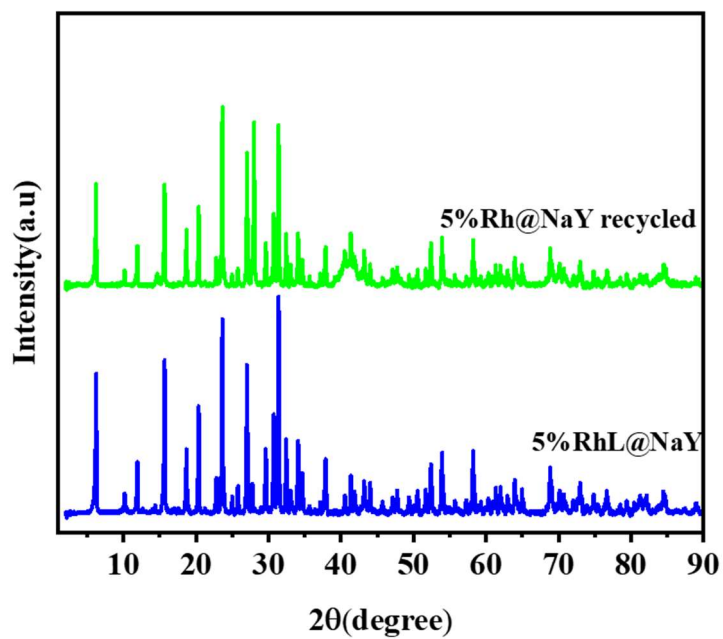


Figure S25. Comparison of the XRD data for the fresh and reused 5%RhL@NaY catalyst.

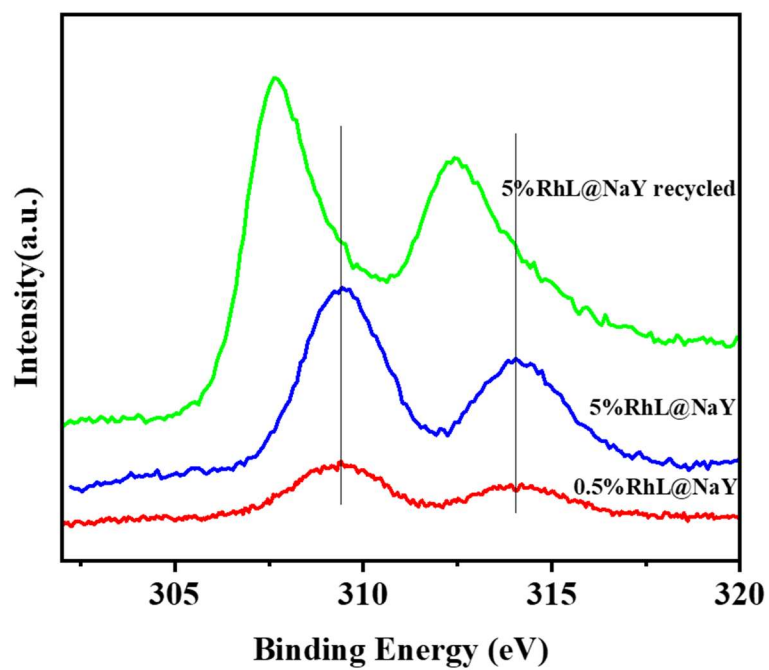


Figure S26. X-ray photoelectron spectroscopy (XPS) comparison data of fresh and recycled 5%RhL@NaY catalyst.

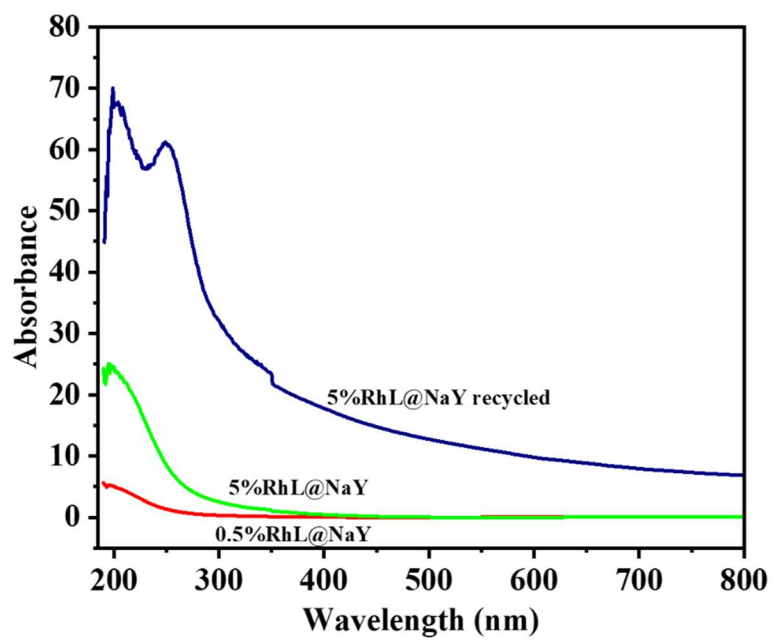


Figure S27. Diffuse-reflectance ultraviolet visible spectrophotometry (DR-UVvis) measurements for 0.5%RhL@NaY, 5%RhL@NaY and used 5%RhL@NaY.

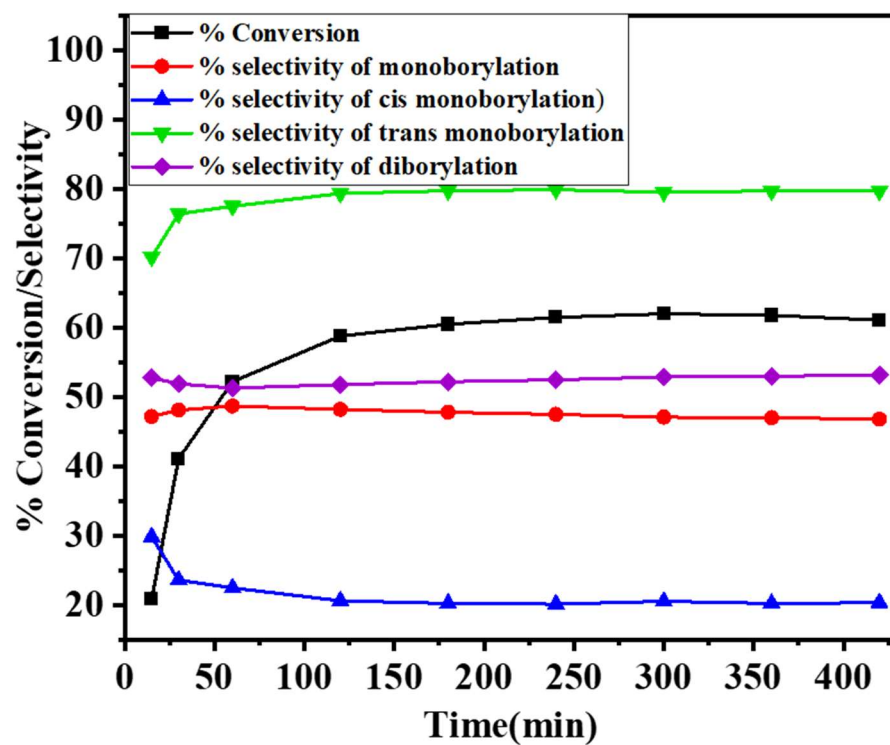


Figure S28. Kinetics for the reaction with 5%RhL@NaY + 6 mol% of XantPhos.